

**Fermi National Accelerator Laboratory**

**FERMILAB-Pub-88/147**

**A Study of the Production and Transport of Muons  
Through Shielding at the TEVATRON\***

J. D. Cossairt, A. J. Elwyn, and W. S. Freeman  
Fermi National Accelerator Laboratory  
P.O. Box 500, Batavia, Illinois 60510

October 10, 1988

\*Submitted to Nucl. Instrum. Methods A



Operated by Universities Research Association Inc. under contract with the United States Department of Energy

# **A STUDY OF THE PRODUCTION AND TRANSPORT OF MUONS THROUGH SHIELDING AT THE TEVATRON**

**J. D. COSSAIRT, A. J. ELWYN, AND W. S. FREEMAN**  
Fermi National Accelerator Laboratory\*  
Batavia, IL 60510, USA

## **ABSTRACT**

The fluence distributions of muons were measured at a number of locations downstream of three different target stations in the fixed-target experimental areas of the Fermilab Tevatron. These were compared with Monte-Carlo calculations of muon production by 800 GeV protons and their transport through shielding materials and regions of magnetic fields. Agreement between the measured and calculated fluence is quite satisfactory at distances between 167 and 3000 meters from the primary production targets. The calculations are therefore a trustworthy tool for predicting muon fluence distributions.

\*Operated by Universities Research Association under contract with the  
U. S. Department of Energy

## 1. Introduction

In Ref. 1, measurements of muon fluence distributions at three locations downstream of the experimental hall of the Tevatron muon beam were described. Comparisons of these measurements with calculations based on the muon transport portion of the Monte-Carlo computer CASIM [2], upgraded for higher energies by Van Ginneken, Yurista, and Yamaguchi [3], were generally satisfactory even after the muons travelled through approximately 2000 meters of earth and air. In this report similar fluence measurements downstream of three other Tevatron experimental area beamlines are described and compared to calculations that include both muon transport mechanisms and muon production models.

In the transport of high energy muons important sources of energy loss include the processes of bremsstrahlung, pair production, and nuclear interactions as well as atomic ionization and excitation. Muon production by relatively low energy protons is dominated by the familiar processes of  $\pi^\pm$  and  $K^\pm$  decay. However, at higher energies mechanisms such as prompt production and direct pair production of  $\mu^+\mu^-$  by  $\pi^0$  in electro-magnetic cascades also must be included. The authors of Ref. 3 have incorporated these additional production mechanisms into their extension of CASIM to higher energy. Muon fluence measurements at various distances downstream of the MP, MC, and MW target stations in the fixed-target experimental areas at Fermilab are compared with calculations obtained using the updated version of

CASIM in a test of the predictive power of this Monte-Carlo program.

## **2. Measurement and Calculation Techniques**

Muon fluence was obtained using a Mobile Environmental Radiation Laboratory (MERL) [4]. Measurements were usually made with a pair of plastic scintillation counters mounted in a vehicle, as discussed in some detail in Ref. 1. In a few places of high muon intensity, a hand-held tissue-equivalent ion chamber was used instead. As in Ref. 1, muon fluence was determined from average background-corrected singles counting rates in the scintillation paddles. At the peaks of the measured fluence distributions, the ratio of coincidence to singles counting rates in the paddles was between 0.6 and 0.8. The results were normalized to the intensity of the proton beam incident on the production targets, determined by secondary emission monitors (SEM's) in the beamlines just upstream of the respective target stations. Measurement errors reported here are based entirely on counting statistics and represent one standard deviation. In the figures that follow, most of these errors are smaller than the symbols used to represent the data points.

Data were obtained at three or more locations downstream of the high energy physics experiments at the MP, MC, and MW beamlines by scanning across the muon radiation field on a line approximately normal to an extension of the beamline. Detector counts were recorded for at least two Tevatron beam spills at each position along a scan. In the

figures that follow, the Z-coordinate is the distance along the beamline measured from the point where the incident proton beam starts to interact with the particle production target. The various positions transverse to the beamline on the fluence scans are described by the X-coordinate in a right-handed Cartesian coordinate system ( $Y > 0$  is vertically upward). The measurements were not dedicated experiments but were carried out during normal operations of the accelerator; this usually included the operation of beams adjacent to the one being studied at a given time. However, on a number of occasions, it was possible to take advantage of periods in which one beam was operating while its neighbor was turned off. The three beams studied are nearly coplanar, are only slightly divergent from each other, and have their production targets at nearly the same longitudinal coordinate. The production targets were separated by about 9 meters laterally. For all measurements there was also some possibility that a small fraction of the detected muons were produced at a known point of beam loss located at about  $Z = -400$  meters.

In the program CASIM, the geometry of interest is specified in a FORTRAN subroutine to a degree of complexity limited principally by the patience of the user. In the present version, as many as five different materials can be used in multi-media calculations. For the calculations done at large distances from the target ( $Z > 450$  meters), air (rather than "vacuum") was explicitly included. For all materials, "standard" values of parameters were chosen. For soil, mostly heavy Illinois clay, the density

was taken to be  $2.25 \text{ g cm}^{-3}$ . Fermilab concrete is typically of density  $2.4 \text{ g cm}^{-3}$ . A number of electromagnets form portions of the beam transport system in the three cases studied. For these, the iron of the magnets (both dipoles and quadrupoles) was always specifically included in the model. For dipoles, the magnetic fields in gaps were included according to the actual operating conditions, while fields in the iron of the magnets were approximated using analytical formulae based upon conservation of magnetic flux. The magnetic fields of the beam transport quadrupoles were ignored. After entry into a soil shield following the experimental hall associated with a given target station, the muons were tracked through it using a data table to determine if the muon was in the dense soil or in the air above the surface.

Modifications to the code of Van Ginneken, et.al. [3] were made to allow calculation of the fluence at specific longitudinal distances. At each selected value of Z, corresponding to a measurement location, a table of muon fluence was generated as a function of X and Y. In order to conserve computer time, a variable step size was used. This parameter is the distance traveled by the hypothetical muon between calculations of the effects of its interaction with matter. The results were found to be insensitive to rather large variations of this parameter. The smaller values were chosen for regions where the geometry involved fine details. A typical calculation to follow the interactions of 2000 incident protons and the resultant muons out to a value of the Z-coordinate of 3000 meters required about 3000 seconds of

CYBER-875 equivalent CPU time. Three different choices of the random number initial value were used to provide an estimate of the error and reproducibility of the calculations. The averages of these three calculations were then compared to the measurements. No "artificial" normalizations were applied to any of these calculations. All comparisons with measurement are on an absolute basis.

#### **4. Beamline Descriptions**

The major features of the target piles for the three Meson Area beams are quite similar, as indicated in Figs 1, 2, and 3. These beams have been described in more detail elsewhere [5,6]. At each station a nuclear target (usually Be) is followed by bending magnets (with magnetic field integrals that vary between 12 and 17 T-m) to deflect the incident protons downward (MP and MC) or horizontally toward negative X-values (MW). Following the magnets at distances between about 10 meters (MC) and 17.5 meters (MP) from the target positions are Cu beam dumps which include collimation designed to transmit desired secondary particles produced at the targets while stopping all primary protons. The collimation is tailored to the requirements of specific high-energy physics experiments. Interactions of the protons in these targets and beam dumps are the dominant sources of muons and their parents. Typical operating intensities are from 1 to  $3 \times 10^{12}$  protons per Tevatron spill. Each spill is of 23 seconds duration repeated approximately once per minute.

Beyond the target piles, the rest of the beamline transport systems for the three beamlines differ in order to meet the requirements of the individual high-energy physics experiments. MP, for example, has a longer drift space between primary target and beam dump than do the other two beamlines, and a second Cu beam dump at a distance of 63 meters from the target. The MP beam contains many large aperture dipoles and is well-shielded by earth, concrete, and steel out to the experimental hall. MC, on the other hand, has few magnetic elements beyond the target station, no earth cover over the beamline, and only local shields of concrete and Fe at isolated locations. MW is as well-shielded as MP out to the experimental hall but has no second beam dump. Furthermore, for MW, there are five toroidal ("spoiler") magnets installed in the beam transport system specifically designed to deflect muons away from the physics experiment (positively-charged particles near the beam are deflected downward). Two of these are very large while three are considerably smaller in cross section. Although these "spoilers" were included in the computer modeling of this geometry, the values of the magnetic field were only crudely approximated as indicated in Fig. 4.

A comparison of the features of the MP, MC, and MW beamlines most relevant to muon production and transport is given in Table 1. The notes to the table describe in a qualitative way the expected impact of these features on the measured muon fluence.

## 5. Results and Discussion

Figure 5 shows the profile of the terrain in the (Y,Z) plane. While this figure actually represents the elevation of the ground surface relative to the MC beam, the topography is very similar for MP and MW. The detailed profile appropriate to each beamline was used in the calculations. These topographical profiles were derived from Fermilab site surveys and United States Geological Survey maps. Approximate locations at which muon fluence was measured are shown on this figure. Comparisons between calculated and measured fluence are presented in order of increasing Z-values in Figures 6 through 10.

The smallest Z-value at which results were obtained is 167 meters ( $Y = 0$  meters) for MC. The results are shown in Fig. 6. The measurement (performed with the hand-held tissue-equivalent chamber) scanned directly across the extension of the primary proton beam directly downstream of the experimental hall. The calculations show reasonably good agreement with the measurements both at the peak and in the tails. Peak centroids (calculated and measured) are at a small value of positive X, which is consistent with the angle at which the incident protons were targeted (as included in the calculations).

At  $Z \approx 375$  meters ( $Y \approx 3$  meters) results are available for all three beams as shown in Fig. 7. (The MP measurements were made with the hand-held tissue-equivalent chamber.) For all three, the calculations describe the measurements at the peaks to within  $\pm 20\%$ . Measured peaks in general tend to be broader than calculated ones. This is

especially notable for MW where the approximation involved in modeling the magnetic fields in the "spoilors" is known to be quite crude. In this figure, the lack of shielding of MC beyond the target station proper is dramatically reflected in a considerably larger peak fluence compared with nearly identical values for the similarly shielded MP and MW beamlines.

Figure 8 compares calculations with measurements taken with hand-held instruments near  $Z \approx 410$  meters ( $Y \approx 9$  meters). The peak fluence at this location on top of a hill (see Fig. 5) is enhanced over the values at  $Z \approx 375$  meters (Fig. 7) because all three of the beamlines incorporate vertically sweeping magnetic fields in their design. The lack of shielding of the secondary beam of MC may cause an additional enhancement to the peak fluence associated with that beam. Agreement with measurement is better for MP and MC than for MW. This, again, may reflect the rather crude modeling of the "spoilors" in the MW beamline.

Results at  $Z \approx 600$  meters ( $Y \approx 0$  meters) are shown in Fig. 9. Here statistical fluctuations in the calculated muon fluence are larger because the fluence is reduced by the greater distance, the earth in the shielding hill, and magnetic dispersion. Variations in the effective attenuation between the three beams may be due to differences in their momentum spectra and phase space distributions. Again, the field due to MC remains the most intense. The calculations describe the measurements within  $\pm 30\%$  even for the least intense field (MP). (The

rise in measured fluence at  $X = 18$  meters in the MP scan is probably due to upstream beam losses not directly related to its operation.) For MW, the agreement is improved, perhaps because this location is less sensitive to details of the modeling of the "spoilers" and relatively more sensitive to the details of the target pile sweeping magnets.

Results obtained at the very large value of  $Z \approx 3000$  meters, ( $Y \approx 3.7$  meters) for MC and MW are shown in Fig. 10. Agreement between the calculations and measurements is still remarkably good, especially for MC.

In any application of the Monte-Carlo technique, one should check the sensitivity to the choice of random number initial value. In Figure 11, the results of the calculations for each of the three selections are compared with each other and the average value for all five measurements done for the MC beamline. It is clear that the results using the different initial values are reasonably consistent with each other even out to  $Z \approx 3$  kilometers.

An additional test of the predictive power of the calculations is provided by comparison with a measured momentum spectrum of muons. At approximately  $Z = 165$  meters, the physics experiment on the MC beamline includes a large magnetic spectrometer system. This device is able to determine the momenta of muons with an efficiency independent of energy above a rather sharp instrumental threshold of about 10 GeV/c. Figure 12 compares a measured spectrum of single muons reported by the experiment with the results of three runs of

CASIM using different initial values of the random number generator. The measurements have been arbitrarily normalized for comparison with the calculations. Agreement in the shape of the spectrum is very good in the region above the instrumental cutoff. The large number of muons predicted below 10 GeV/c may account for the difference between the MC fluence measurements and those of MP. For MP, muons of such low momentum may be ranged out by the additional earth shielding resulting in a lower fluence. No comparable shielding is present in the MC beamline.

## **7. Summary and Acknowledgement**

The results indicate that the CASIM Monte-Carlo program for describing both the production of muons and their transport in shields of considerable complexity does an excellent job of predicting distributions of muon fluence without the application of arbitrary normalization factors. Agreement of the calculations with measurements of the distributions is often within 20 per cent near peaks and generally within a factor of two elsewhere. This agreement remains good over large distances for realistic complex shielding geometries, and with less than perfect knowledge of the magnetic field at all spatial coordinates within magnets.

We would like to thank R. Coleman for his helpful discussions of the operation of these beams and J. Larson and T. Anderson for their skill in maintaining reliable operation of the apparatus. Special thanks

are due to A. Van Ginneken for making the extended CASIM program available to us and for many helpful discussions.

**References**

1. J. D. Cossairt, A. J. Elwyn, W. S. Freeman, and S. W. Butala, submitted for publication in Nucl. Instr. and Meth.
2. A. Van Ginneken and M. Awschalom, High Energy Particle Interactions in Large Targets (1975), Fermi National Accelerator Laboratory, Batavia, Illinois, USA) and A. Van Ginneken; Fermilab Report FN-272 (1975), Fermi National Accelerator Laboratory, Batavia, Illinois, USA.
3. A. Van Ginneken, P. Yurista, and C. Yamaguchi, Fermilab Report FN-447 (1987), Fermi National Accelerator Laboratory, Batavia IL 60510, USA.
4. J. D. Cossairt, Health Physics 45 (1981) 651.
5. Tevatron II Facilities Handbook, (1986), Fermi National Accelerator Laboratory, Batavia, IL 60510, USA.
6. Fermilab Research Program 1987, R. Rubenstein, Editor (1987), Fermi National Accelerator Laboratory, Batavia, IL 60510, USA.

Table 1 Features of beamline configurations expected to be important with respect to muon production and transport

Feature	MP	MC	MW
drift space between primary target and beam dump <sup>a</sup>	longest	shortest	medium
separate beam dump for secondaries <sup>b</sup>	yes	no	no
deflection of positives after primary target <sup>c</sup>	downward	downward	rightward
earth shielding of secondary beamline <sup>d</sup>	yes	no	yes
deflection of muons by large magnets <sup>e</sup>	yes	no	yes

Notes:

- a) A longer drift space between the primary target and the primary beam dump used to absorb the incident protons should increase the number of muons resulting from  $\pi$  and K decay.
- b) A separate beam dump for a large flux of secondary particles could present an additional source of muons.
- c) Vertical deflection after the primary target could reduce the fluence in the horizontal plane of the beam while increasing it above and below it.
- d) Earth shielding over the secondary beamline should serve to reduce the fluence of the lower momenta muons.
- e) The presence of large magnets in the secondary beamline should reduce their number by dispersing them over large areas.

### List of Figure Captions

1. Plan and cross-sectional elevation views of the MP target station and its associated secondary and tertiary beamline. The earth-shielded beam enclosure continues on to an experimental hall beginning at  $Z = 310$  meters.
2. Plan and cross-sectional elevation views of the MC target station and its associated secondary beamline. Additional "local" shields of concrete and steel were included in the calculations but are not shown in the figure.
3. Plan and cross-sectional elevation views of the MW target station and its associated secondary beamline. The earth-shielded beam enclosure continues on to an experimental hall beginning at  $Z = 311$  meters. Only the two larger muon "spoilers" are shown in the figure. The three smaller ones are located at larger values of  $Z$ .
4. Cross sections for two of the five muon "spoiler" magnets used in the MW secondary beam. Idealized values of magnetic fields are shown in the various sections of the magnet iron. The other large "spoiler" (3.5 meters long) is similar, but somewhat larger in cross section than the large "spoiler" shown here. All three of the small "spoilers" are identical.

5. Plot of the surface topography relative to the beam elevation as a function of Z for the MC target station and its associated beamline. The lower frame is a magnification of the region near the shielding hill. The terrain profiles for the MP and MW beamlines are similar. The filled symbols indicate approximate locations where muon fluence measurements were made.
6. Measurements (filled symbols) and calculations (solid line) of the muon fluence as a function of X for the MC beam at Z = 167 meters, Y = 0.0 meters. The units of muon fluence are  $\text{cm}^{-2}$  per  $10^{12}$  incident protons.
7. Measurements (filled symbols) and calculations (solid line) of the muon fluence as a function of X for the MP beam at Z = 378 meters, Y = 3.2 meters (top), the MC beam at Z = 373 meters, Y = 2.7 meters (center), and the MW beam at Z = 381 meters, Y = 3.0 meters (bottom). The units of muon fluence are  $\text{cm}^{-2}$  per  $10^{12}$  incident protons.
8. Measurements (filled symbols) and calculations (solid line) of the muon fluence as a function of X for the MP beam at Z = 420 meters, Y = 9.8 meters (top), the MC beam at Z = 402 meters, Y = 9.9 meters (center), and the MW beam at Z = 406 meters, Y = 8.5 meters (bottom). The units of muon fluence are  $\text{cm}^{-2}$  per  $10^{12}$  incident

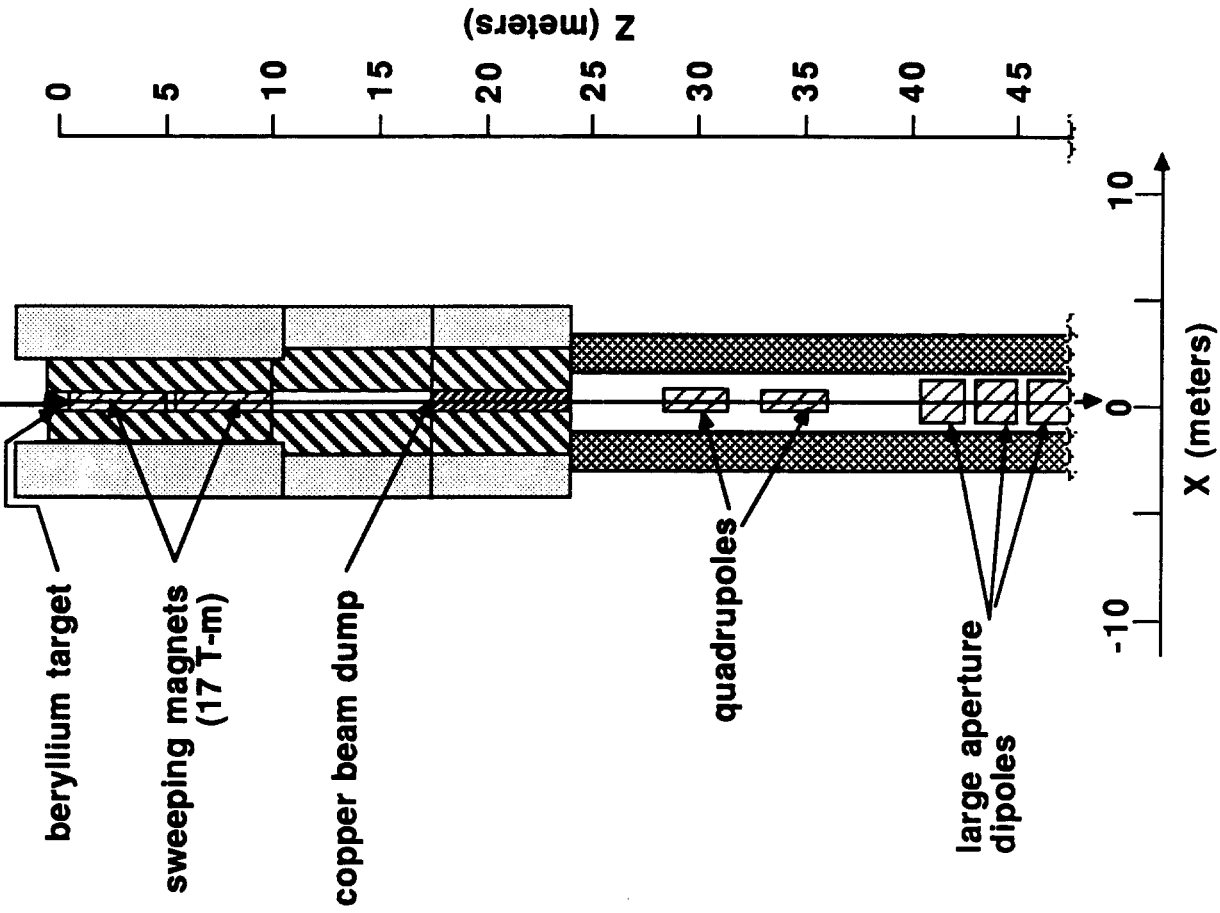
protons.

9. Measurements (filled symbols) and calculations (solid line) of the muon fluence as a function of X for the MP beam at Z = 642 meters, Y = -0.9 meters (top), the MC beam at Z = 600 meters, Y = -0.6 meters (center), and the MW beam at Z = 590 meters, Y = -0.6 meters (bottom). The units of muon fluence are  $\text{cm}^{-2}$  per  $10^{12}$  incident protons.
10. Measurements (filled symbols) and calculations (solid line) of the muon fluence as a function of X for the MC beam at Z = 2900 meters, Y = 3.7 meters (top) and the MW beam at Z = 3000 meters, Y = 3.7 meters (bottom). The units of muon fluence are  $\text{cm}^{-2}$  per  $10^{12}$  incident protons.
11. Monte-Carlo results of muon fluence (ordinate) in units of  $\text{cm}^{-2}$  per  $10^{12}$  incident protons as a function of X (abscissa) in units of meters for three choices of random number initial value (open symbols) compared with their average (solid line) for each Z-value at which measurements were obtained for the MC beamline.
12. Calculations of the muon momentum spectrum at Z = 165 meters compared with results obtained by the high energy physics experiment which used the MC beam. Three different random

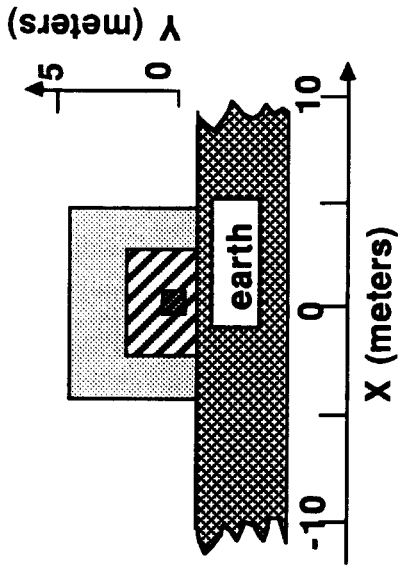
number initial values (broken line histograms) and their average (solid histogram) are shown. The calculations were summed over the spatial region corresponding to the aperture of the spectrometer.

**PLAN VIEW IN BEAM PLANE:**

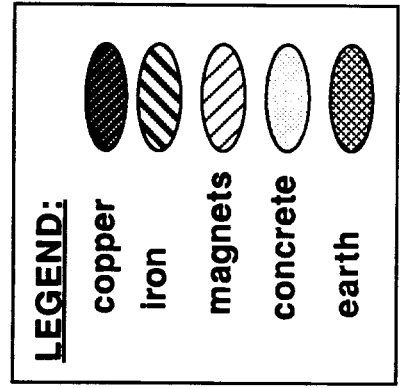
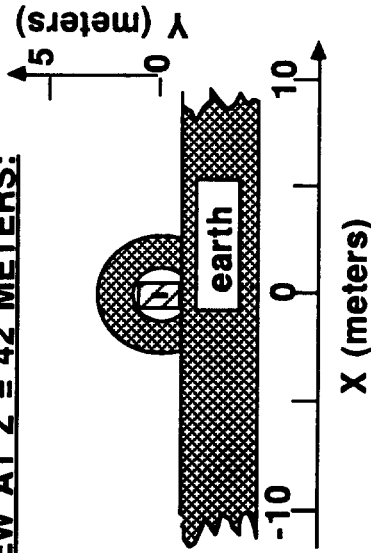
800 GeV proton beam



**ELEVATION VIEW AT Z = 20 METERS:**



**ELEVATION VIEW AT Z = 42 METERS:**



**MP BEAMLINE**

Figure 1

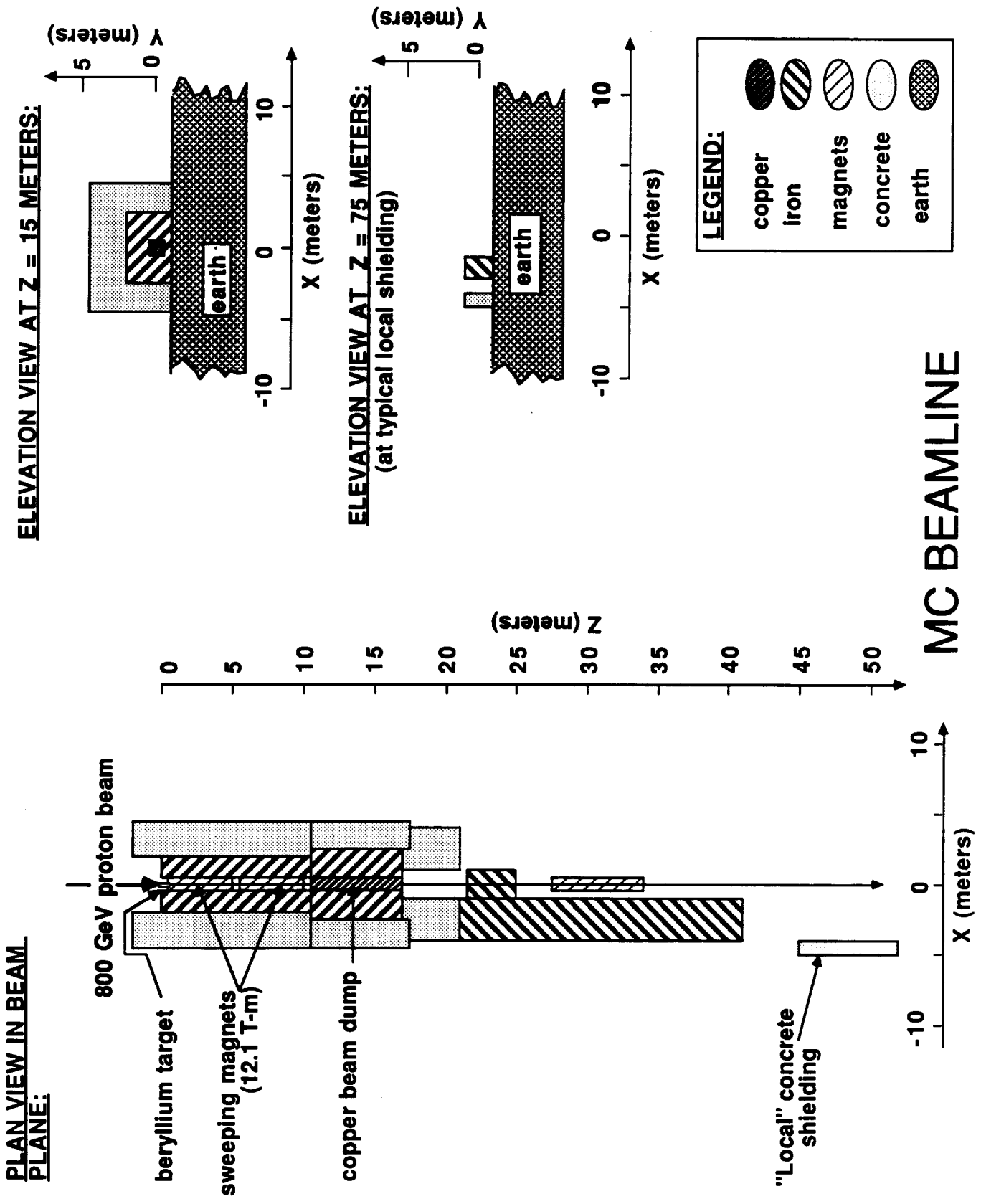
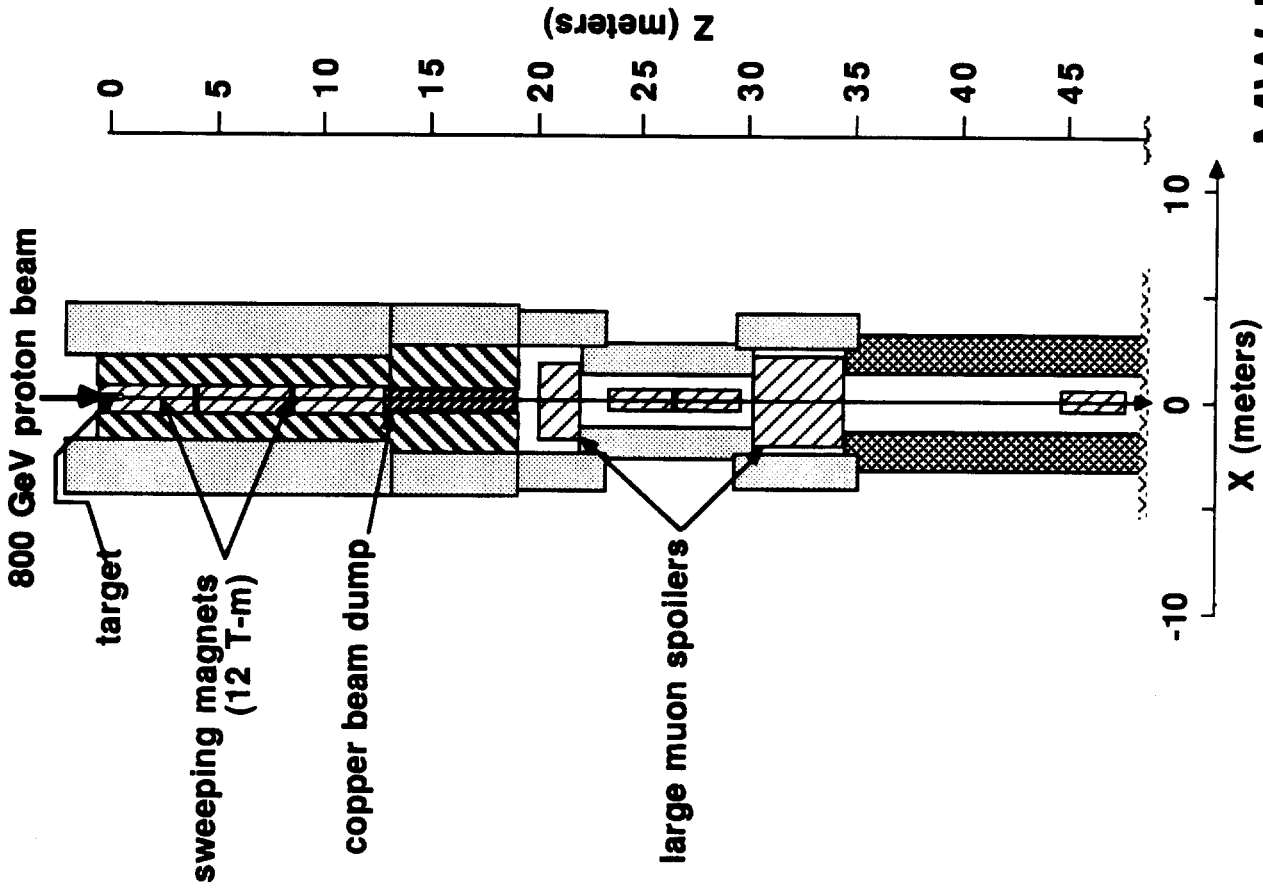
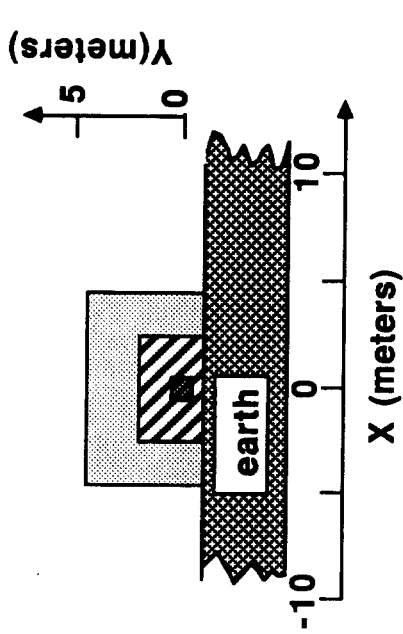


Figure 2

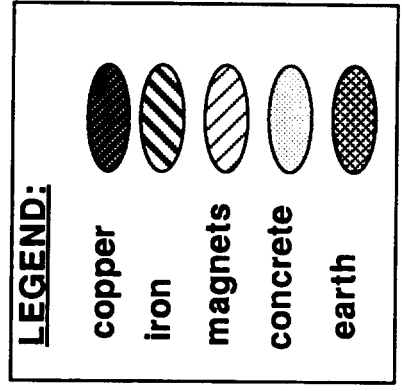
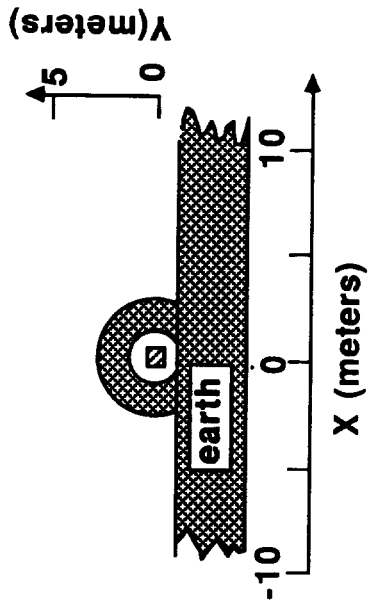
**PLAN VIEW IN BEAM PLANE:**



**ELEVATION VIEW AT Z = 15 METERS:**



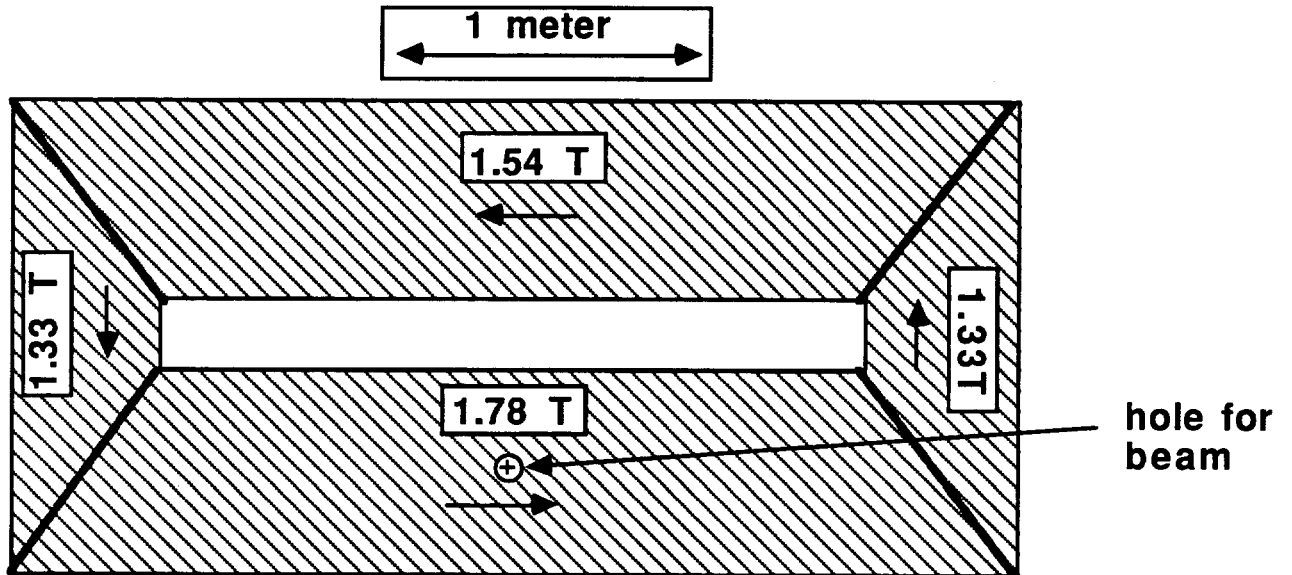
**ELEVATION VIEW AT Z = 25 METERS:**



**MW BEAMLINE**

Figure 3

**LARGE MUON SPOILER (2.1 m long):**



**SMALL MUON SPOILER (6.1 m long):**

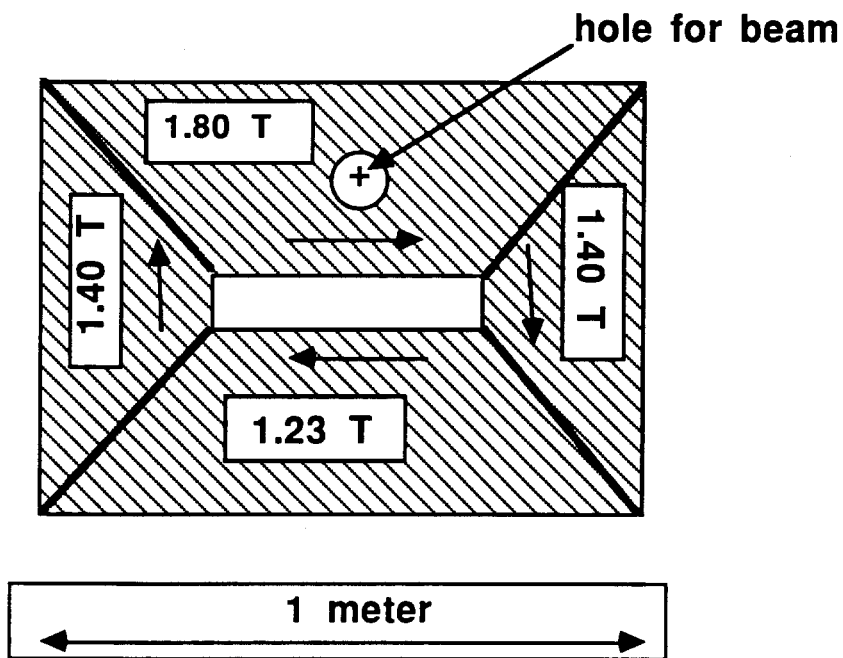


Figure 4

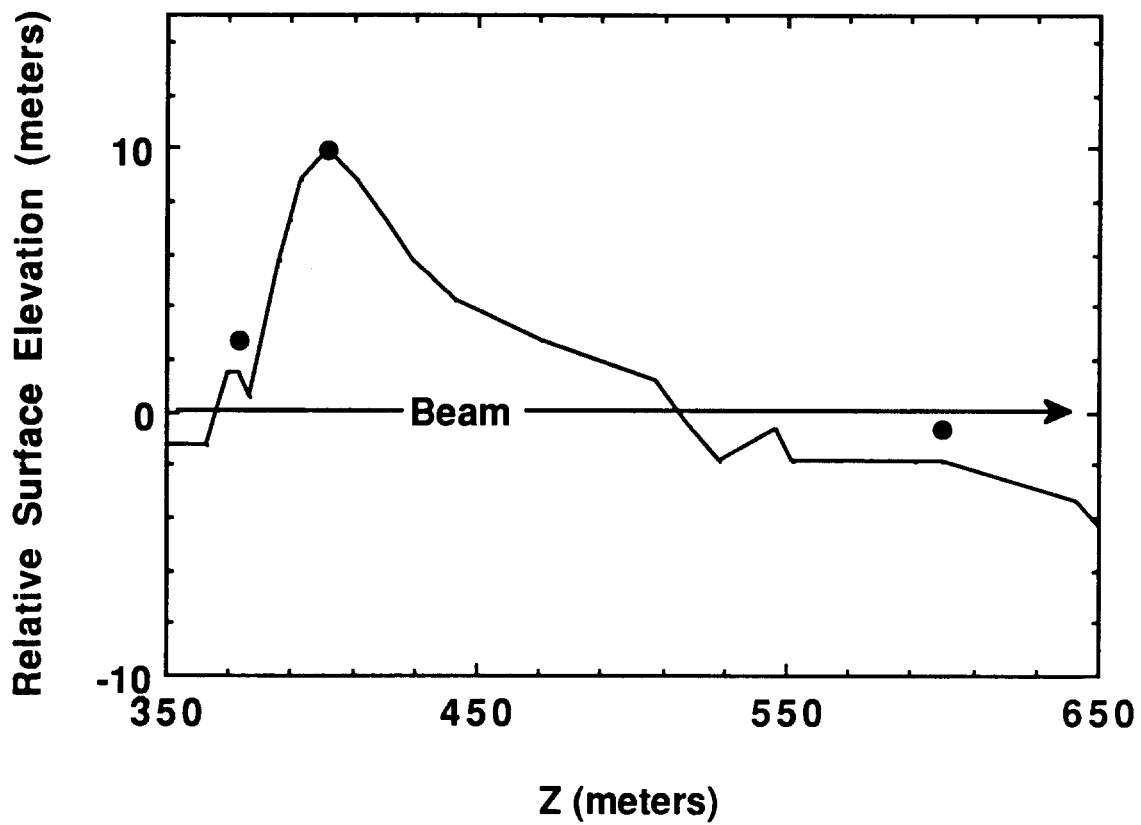
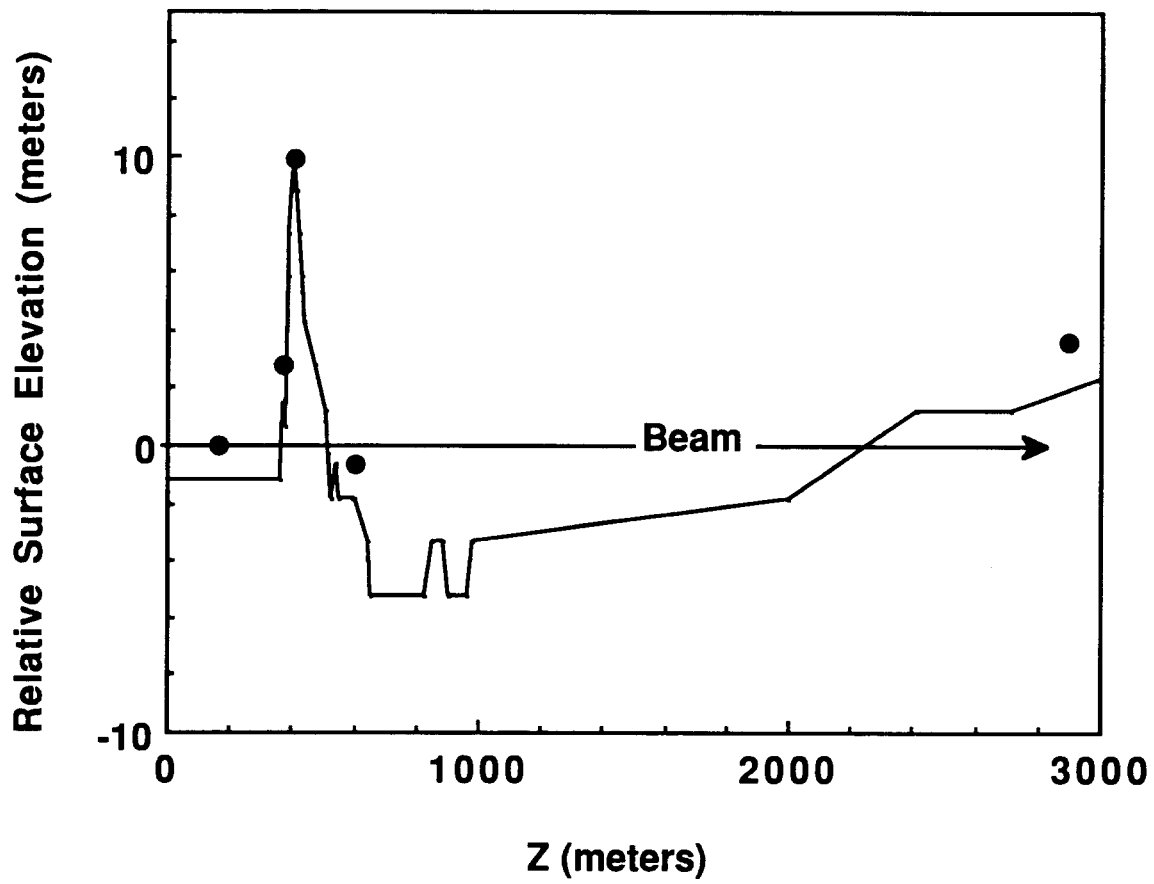


Figure 5

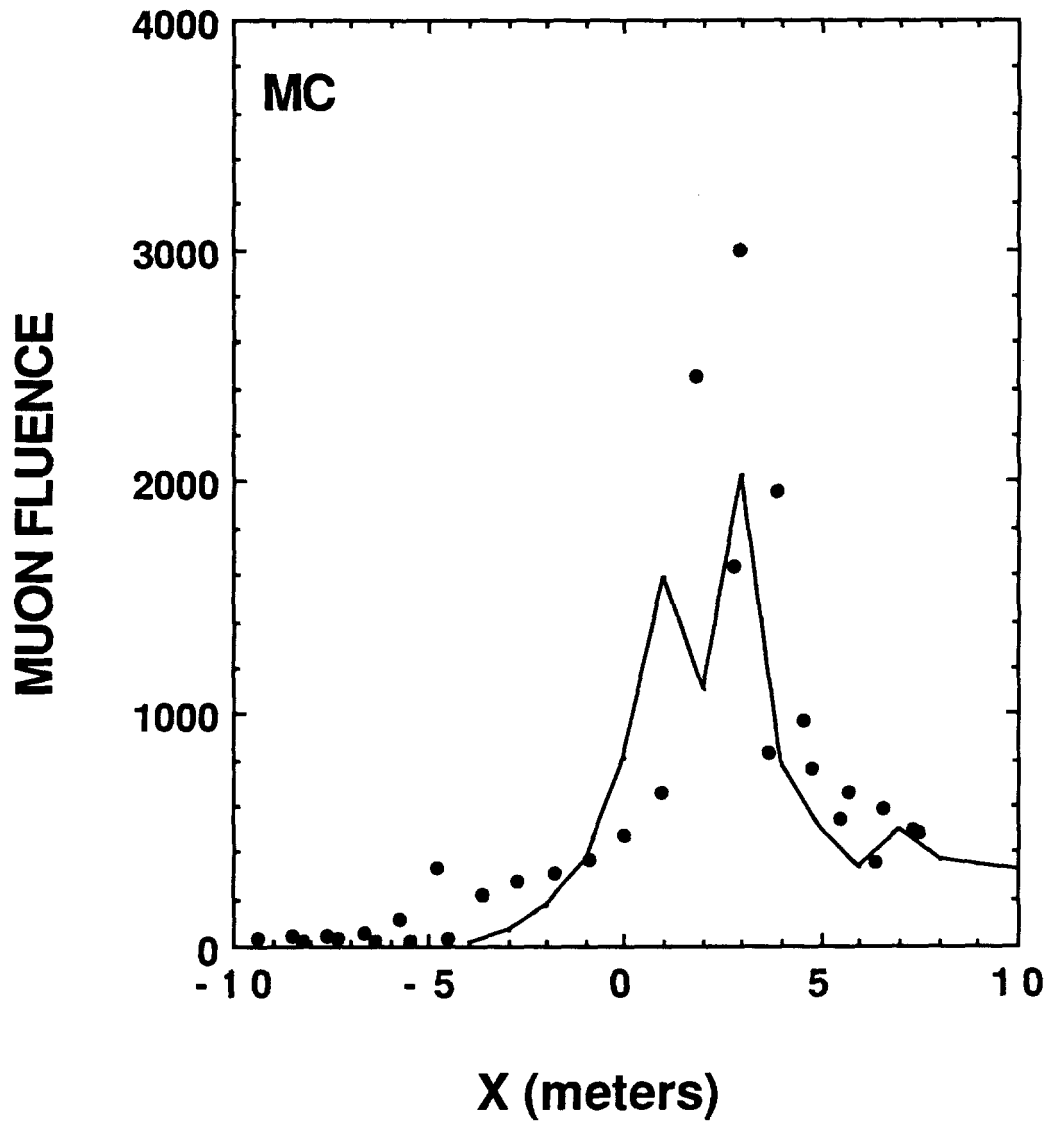


Figure 6

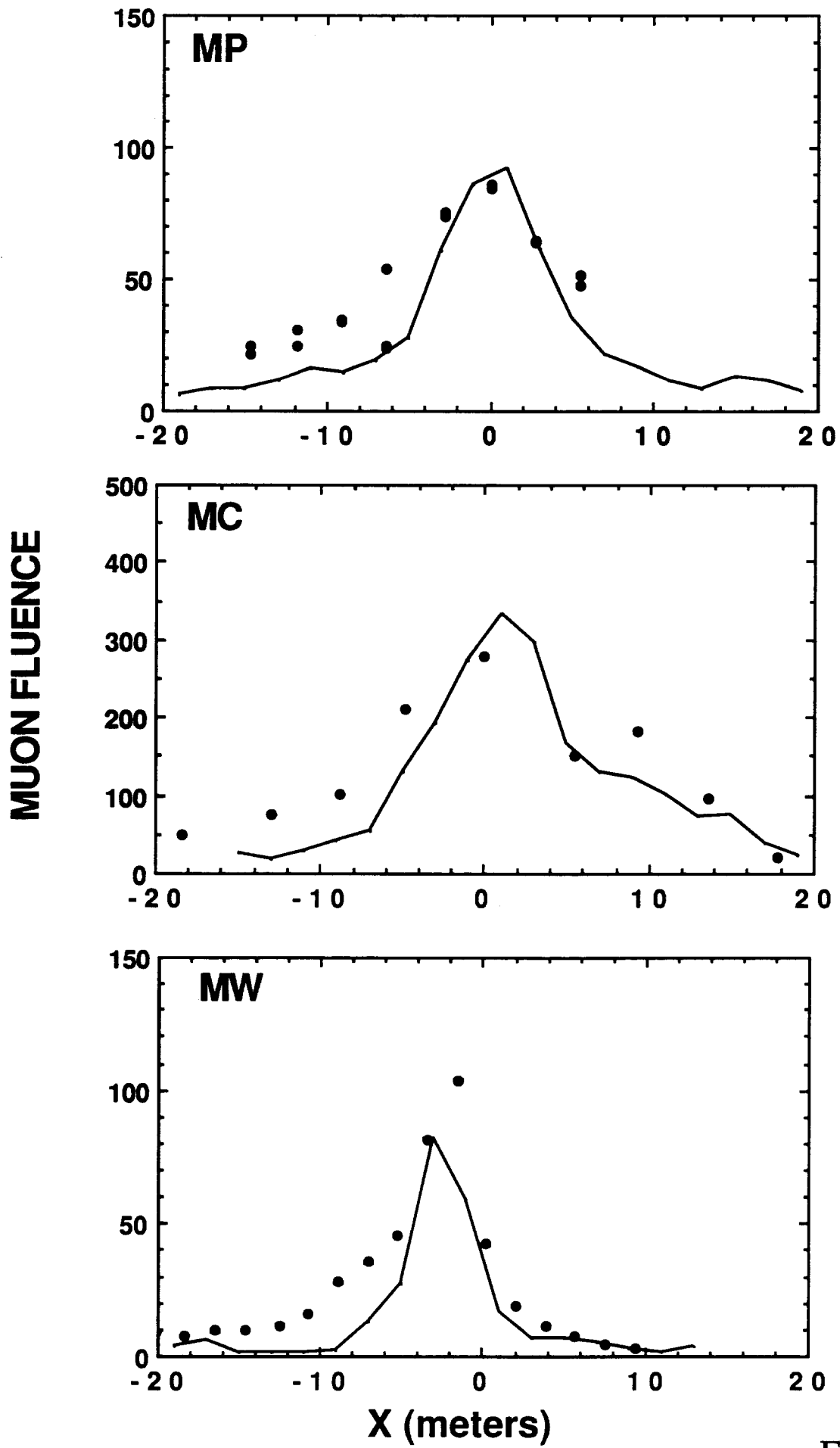


Figure 7

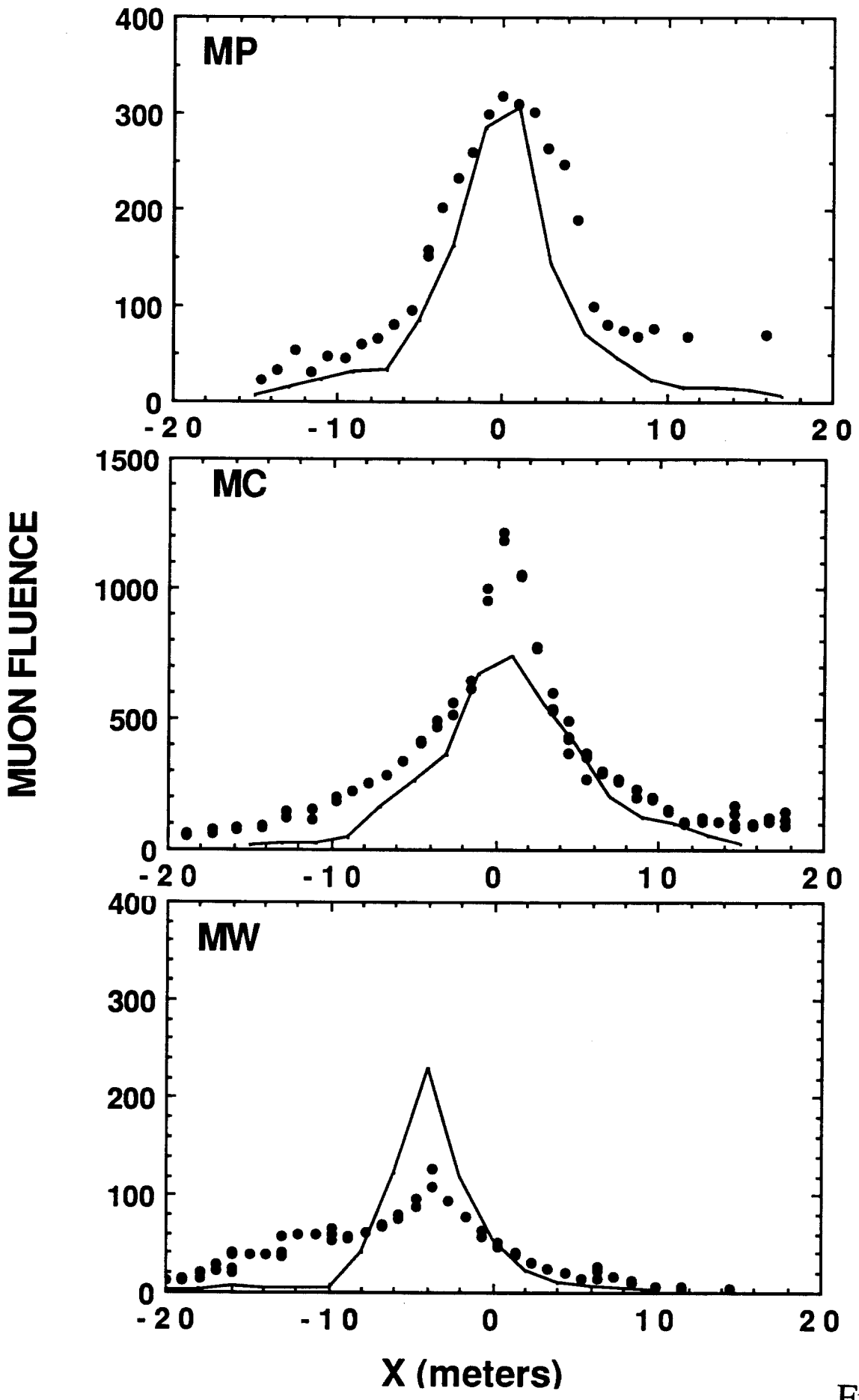


Figure 8

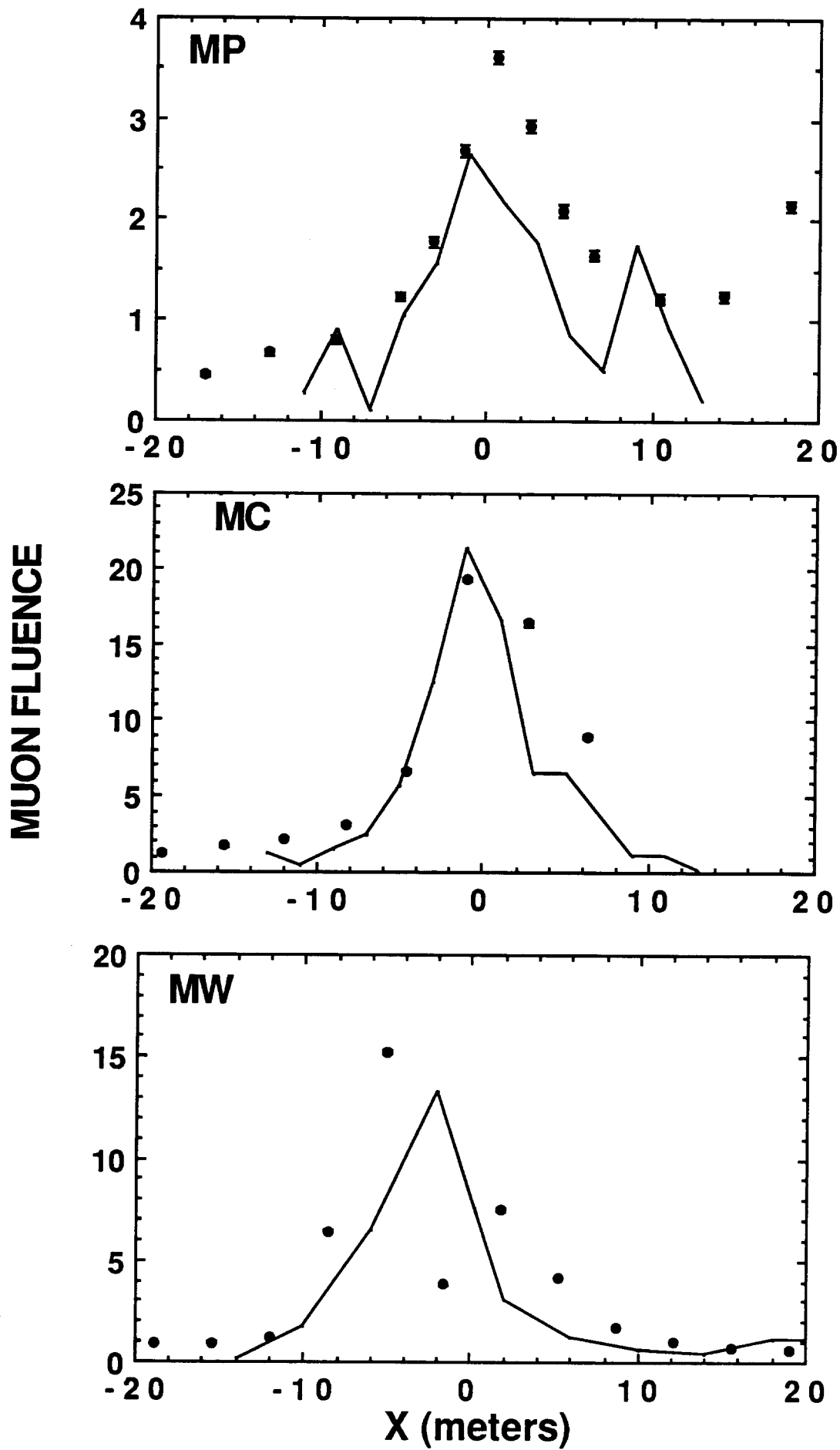


Figure 9

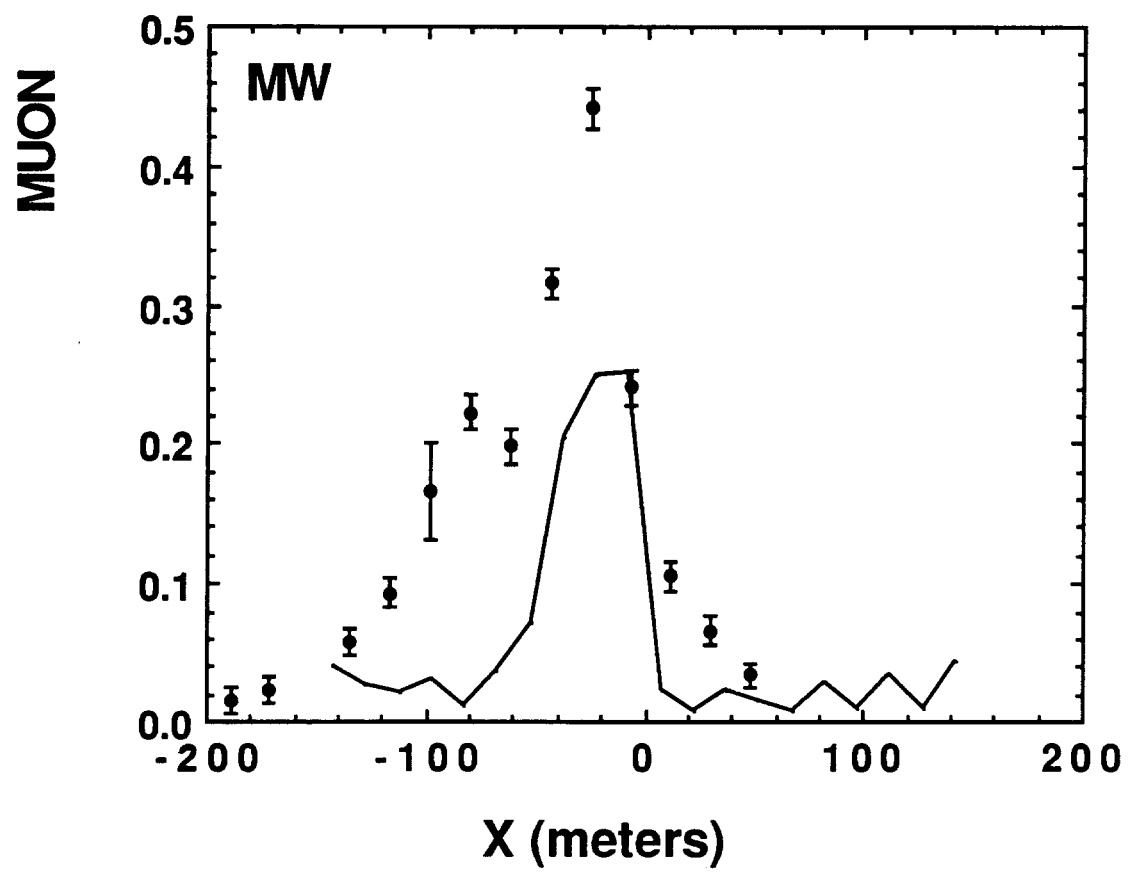
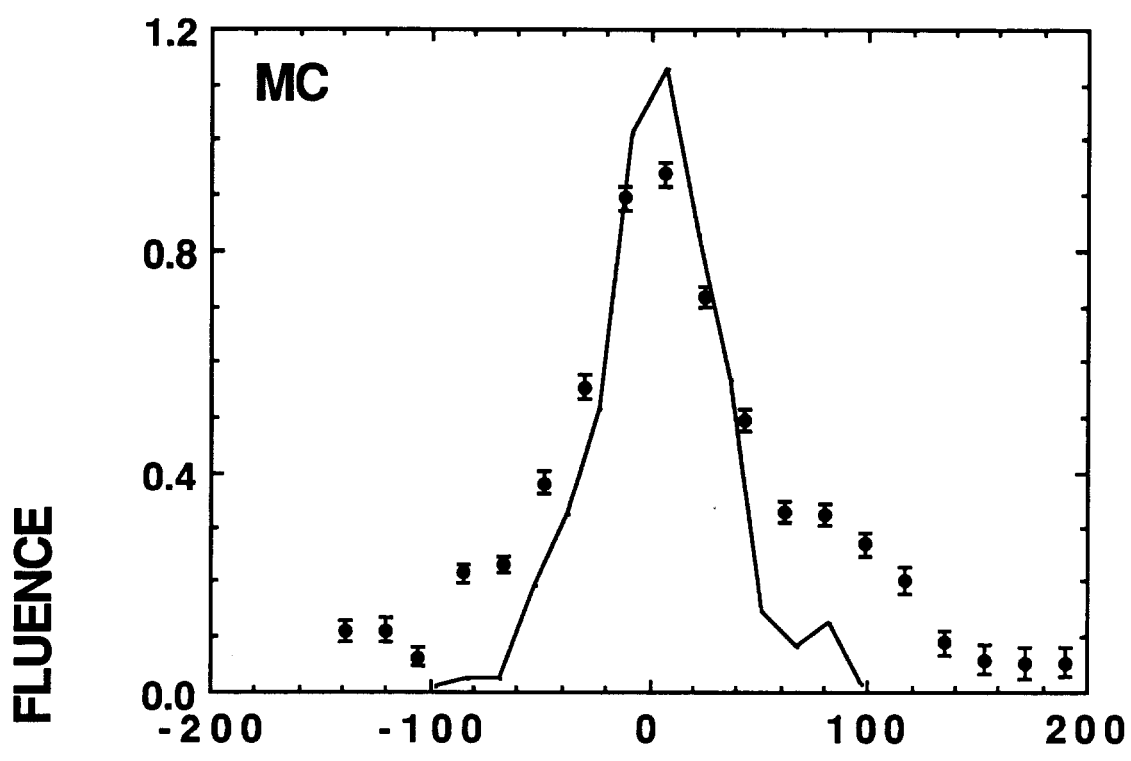


Figure 10

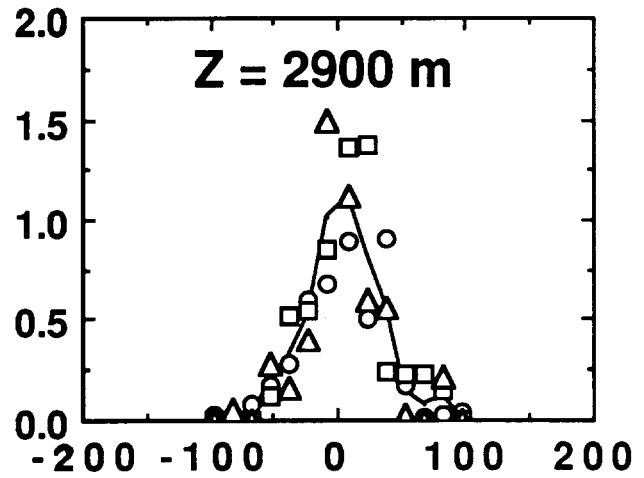
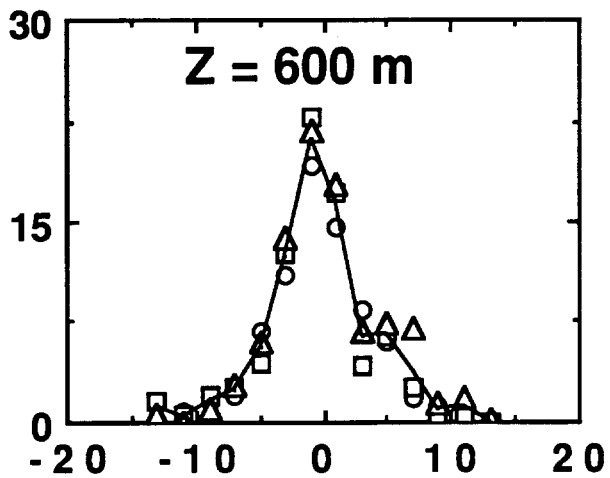
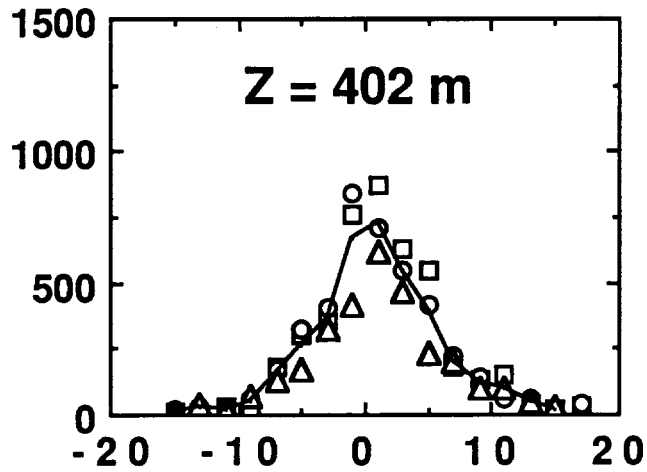
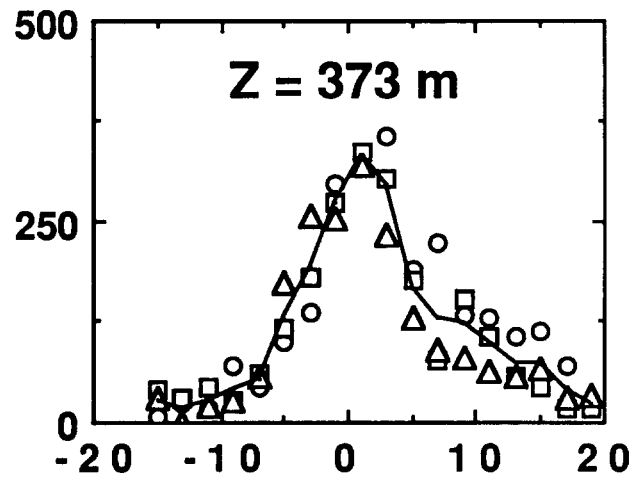
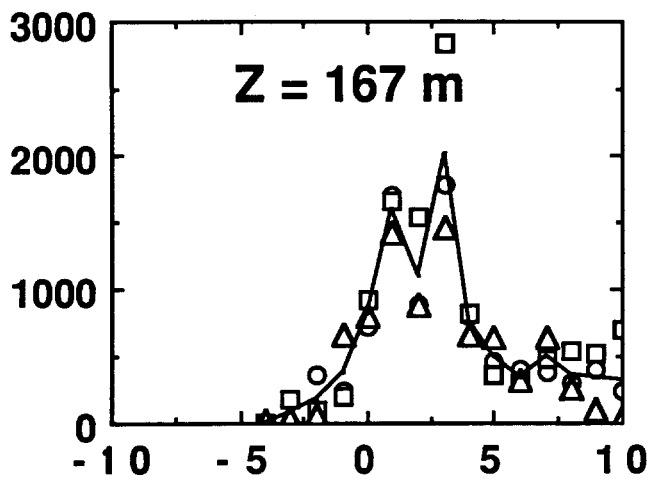


Figure 11

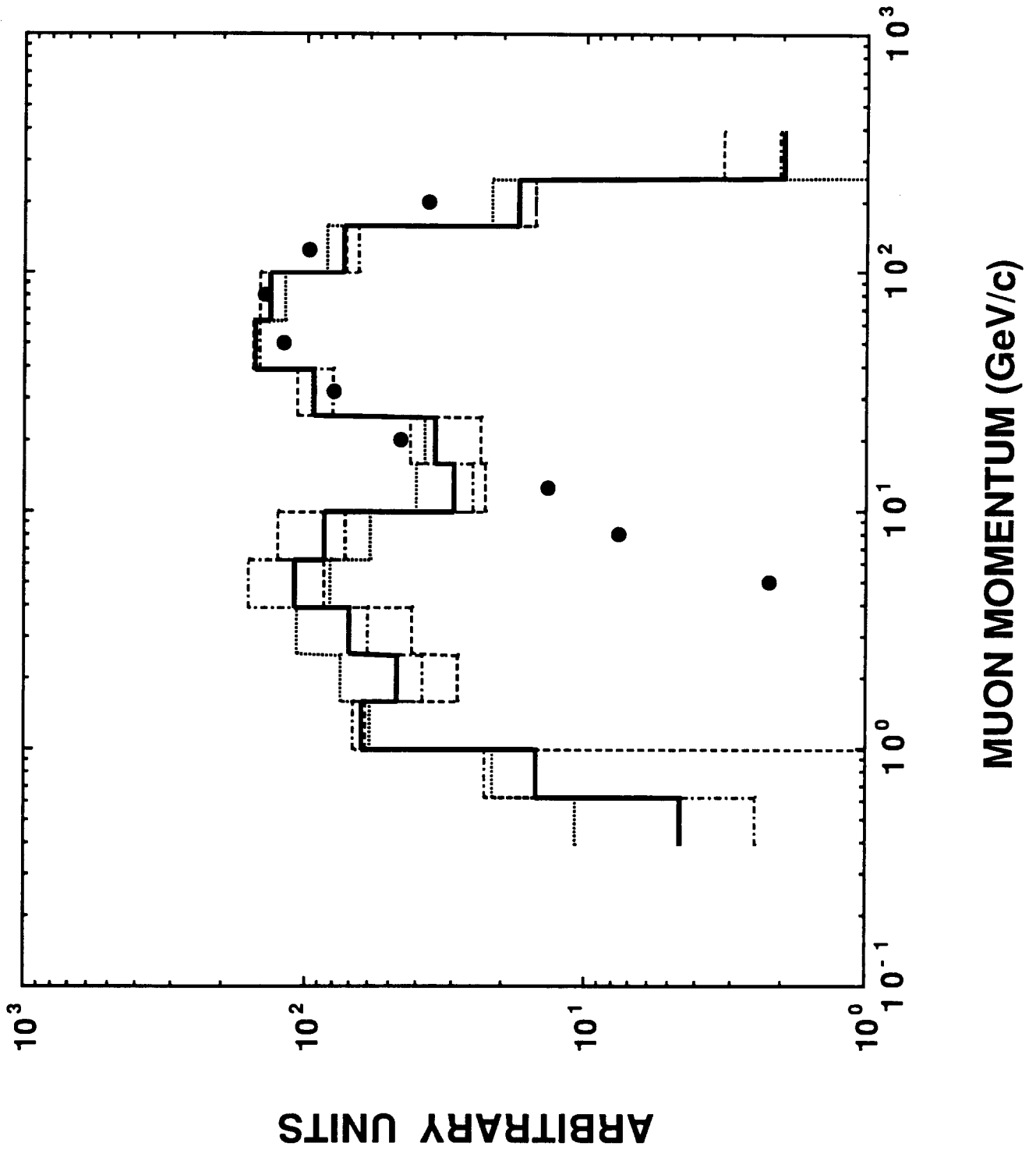


Figure 12